Screened exchange dynamical mean field theory and its relation to density functional theory: $SrVO_3$ and $SrTiO_3$

Ambroise van Roekeghem[1,2] [(a)] and Silke Biermann[2,3,4,5] [(b)]

[1] *Beijing National Laboratory for Condensed Matter Physics, and Institute of Physics, Chinese Academy of Sciences, Beijing 100190, China*
[2] *Centre de Physique Théorique, Ecole Polytechnique, CNRS UMR 7644, 91128 Palaiseau, France*
[3] *Collège de France, 11 place Marcelin Berthelot, 75005 Paris, France*
[4] *European Theoretical Synchrotron Facility, Europe*
[5] *Kavli Institute for Theoretical Physics, University of California, Santa Barbara, California 93106, USA*

arXiv:1412.7971v1 [cond-mat.str-el] 26 Dec 2014

PACS 71.15.-m – Methods of electronic structure calculations
PACS 71.27.+a – Strongly correlated electron systems; heavy fermions
PACS 71.10.-w – Theories and models of many-electron systems

Abstract –We present the first application of a recently proposed electronic structure scheme to transition metal oxides: screened exchange dynamical mean field theory includes non-local exchange beyond the local density approximation and dynamical correlations beyond standard dynamical mean field theory. Our results for the spectral function of $SrVO_3$ are in agreement with available experimental data, including photoemission spectroscopy and thermodynamics. Finally, the $3d^0$ compound $SrTiO_3$ serves as a test case to illustrate how the theory reduces to the band structure of standard electronic structure techniques for weakly correlated compounds.

Introduction. – Combined density functional many body theories, such as the combination of the local density approximation with dynamical mean field theory ("LDA+DMFT") [1–3], have revolutionized the field of first principles electronic structure calculations over the last decade, and many successful applications to materials ranging from simple transition metals [4, 5] or f-electron metals [6–8] to complex oxides [9, 10] have been worked out. Nevertheless, it has also been pointed out that conceptual deficiencies related to the use of the Kohn-Sham band structure or the neglect of dynamical screening effects [11–13] may have practical implications limiting the predictive power of the approach. A more satisfactory approach, formulated entirely in a Green's function language, is the combined many-body perturbation dynamical mean field theory scheme "GW+DMFT" [14–16]. The first implementations of GW+DMFT have recently been elaborated, with applications to $SrVO_3$ [17,18] and to systems of adatoms on surfaces [19]. Nevertheless, since the approach is computationally heavy, an important line of research remains the developing and testing of approximate schemes, and several different simplified schemes [20–22] have recently appeared.

Here, we focus on the recently proposed "Screened Exchange Dynamical Mean Field Theory" [22], where a one-particle Hamiltonian beyond DFT-LDA is constructed and supplemented by a many-body self-energy calculated from DMFT with frequency-dependent local Hubbard interactions. We apply this new method to the transition metal oxide $SrVO_3$, a moderately correlated metallic compound which – thanks to its simple electronic structure – has become a benchmark compound for DMFT-based methods. The results are in agreement with the available experimental information stemming from angle-resolved and angle-integrated photoemission spectroscopy, optics and thermodynamics. We confirm a striking band-widening effect in the unoccupied part of the electronic structure, recently discovered within GW+DMFT [18], and which urgently calls for investigations by inverse photoemission or related techniques. Finally, we apply our scheme to the weakly correlated band insulator $SrTiO_3$: here, a most interesting cancellation of band widening by screened exchange and dynamical effects elucidates the relation of the new technique to standard Density Functional Theory (DFT) or GW techniques. Using (lightly doped) $SrTiO_3$ as a

[(a)] E-mail: vanroeke@cpht.polytechnique.fr
[(b)] E-mail: biermann@cpht.polytechnique.fr

prototype we argue that Screened Exchange Dynamical Mean Field Theory reproduces the band structure of the standard theories for materials with weak correlations.

Screened exchange dynamical mean field theory. – Combining screened exchange with dynamical mean field theory with frequency-dependent interactions ("dynamical DMFT" or "DDMFT") brings in two important corrections, as compared to standard LDA+DMFT, namely (1) non-local exchange beyond the LDA and (2) dynamical screening beyond usual DMFT. The scheme can be understood as a simplified version of combined "GW+DMFT" or as a dynamical non-perturbative generalization of Hedin's COulomb-Hole-Screened-EXchange (COHSEX) approximation [23]. From a functional point of view, it corresponds to replacing the screened Coulomb interaction in the nonlocal part of the GW+DMFT functional (see e.g. Eq. (4) in Ref. [14]) by its zero-frequency value. In practice, in the recently implemented combined "Screened Exchange plus Dynamical DMFT" (SEx+DDMFT) scheme [22], a one-particle Hamiltonian is constructed as

$$H_0 = H_{Hartree} + H_{SEx} = H_{LDA} - V_{xc}^{LDA} + H_{SEx} \quad (1)$$

where H_{SEx} is a screened Fock exchange term, calculated from the Yukawa potential

$$\frac{e^2 exp(-k_{TF}|r-r'|)}{|r-r'|} \quad (2)$$

with screening wavevector k_{TF}. The latter is self-consistently calculated from the spectral function at the Fermi level. The density used in the construction of H_0 is taken to be the converged DFT-LDA one. The underlying rationale of this choice is the observation that DFT-LDA densities are often extremely close to the true densities, even when the Kohn-Sham band structure is not a good approximation to spectral excitations.

The many-body part of the Hamiltonian

$$H_{int} = H_{int\ stat} + H_{screening} \quad (3)$$

contains two terms: (1) static two-body interactions

$$H_{int\ stat} = \frac{1}{2}\sum_i \sum_{m\sigma \neq m'\sigma'} V_{m\sigma m'\sigma'} n_{im\sigma} n_{im'\sigma'} \quad (4)$$

as in usual LDA+DMFT, but with the *bare* Coulomb interaction matrix V incorporating Hubbard interactions and Hund's coupling. The sums m, m' run over the correlated orbitals, that is, in our case the t_{2g} states of $SrVO_3$, localized at atomic sites labeled by i.
(2) Dynamical screening as described by introducing a set of auxiliary screening bosons (creation and annihilation operators $b^\dagger$ and b), coupling to the physical electrons:

$$\begin{aligned} H_{screening} &= \sum_i \int_\omega d\omega \left[\lambda_\omega \sum_{m\sigma} n_{im\sigma} (b^\dagger_{i,\omega} + b_{i,\omega}) \right. \\ &+ \left. \omega \left(b^\dagger_{i,\omega} b_{i,\omega} + \frac{1}{2} \right) \right]. \end{aligned} \quad (5)$$

The set of screening bosons can be understood as a parametrization of local dynamical Coulomb interactions $\mathcal{U}(\omega)$, as recently introduced in dynamical DMFT calculations [12]. Physically, these bosonic screening modes describe plasmons or particle-hole excitations, which reduce the initial Coulomb interaction at low-energies, making the effective interaction a frequency-dependent (retarded) quantity. The final Hamiltonian $H = H_0 + H_{int}$ has the form of a multi-orbital Hubbard-Holstein Hamiltonian, which we treat within dynamical mean field theory, using a continuous-time hybridization expansion Monte Carlo solver [24]. In this work, we use the recent implementation of Ref. [22].

In our applications to $SrVO_3$ and $SrTiO_3$ below, we focus on the t_{2g}-states only, thus dealing with a three-fold degenerate dynamical impurity problem. Calculations are performed on the imaginary time axis at a temperature T = 400 K, and analytically continued to obtain spectral functions by means of a Maximum Entropy scheme [25].

Due to the degenerate nature of the t_{2g}-states an important simplification occurs for the self-consistent calculation of the screening wavevector: indeed, Luttinger's theorem prevents any modifications of the spectral function on the Fermi level by a local self-energy (other than temperature-induced changes which are tiny in our case). Therefore, the self-consistent value of the screening wavevector can already be obtained from the result of the SEx calculation, resulting in $k_{TF} = 1.1\ a_0^{-1}$.

$SrVO_3$, a correlated metal. – $SrVO_3$ has become a classical "drosophila" compound in the field of electronic structure calculations for correlated materials. The reason is easy to see: the perfect cubic crystal structure of this d^1 compound results in a crystal field that lifts the five-fold degeneracy of the V-3d states, leaving only the t_{2g}-states at the Fermi level. The low-energy electronic structure is thus of appealing simplicity with a single electron in a manifold of three perfectly degenerate t_{2g}-states. Transport measurements have early on pointed out a surprisingly large Fermi liquid regime, extending practically up to room temperature [26]. Due to the relatively localized nature of the corresponding orbitals and a non-negligible Coulomb interaction, the spectral properties are however not well-described by simple band theory. Various experimental probes, in particular photoemission [27–32], inverse photoemission [33] and angle-resolved photoemission [34–37] have been used to characterize the spectral properties of this compound. The resulting picture is that of a moderately correlated metal, with quasi-particle mass enhancement of the order of 2 and a well-defined lower Hubbard band that has been identified in various spectroscopic probes.

Electronic structure calculations have been able to reproduce this correlated metal behavior, and the study of the weight transfer between quasi-particle states and the lower Hubbard band has been one of the early achievements of LDA+DMFT [27,38,39]. Later on, more refined

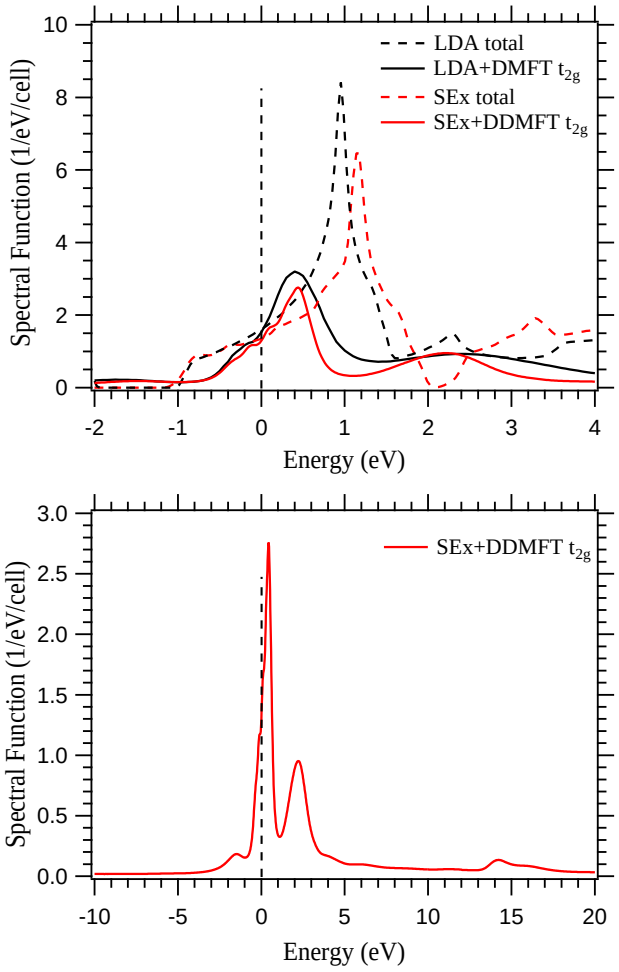

Fig. 1: Momentum-integrated spectral function of the t_{2g} states of $SrVO_3$ within SEx+DDMFT. Also given on the upper panel is the spectral function of the t_{2g} states from standard LDA+DMFT with U=4.0, reproduced from [42], the LDA total density of states and the SEx total density of states. The larger energy scale in the lower panel allows us to identify also the peaks due to the plasmon excitation at 15 eV.

details of the electronic structure such as possible kink structures in the low-energy electronic spectra [40] or non-local correlations [41] have also come into focus.

Despite the seemingly well-understood physics of $SrVO_3$, the recent application of combined GW+DMFT reserved however new surprises: it was found, for example, that a prominent peak observed in inverse photoemission and usually interpreted as an upper Hubbard band of t_{2g}-character should be dominantly attributed to the e_g-states [18]. The true upper Hubbard band is in fact located at much lower energies, such that it merges with the quasi-particle band structure observed in inverse photoemission.

A rather detailed overview of the experimental and theoretical investigations has recently been given in Ref. [18].

We now turn to the discussion of our results for $SrVO_3$ within SEx+DDMFT. The momentum-integrated spectral function (Fig. 1) displays a three-peak structure – a renormalized quasi-particle peak and Hubbard bands – as in LDA+DMFT. Indeed, in the occupied part of the spectrum the picture is very close to the LDA+DMFT one. For positive energies, however, significant differences are observed: the upper Hubbard band is located at about 2 eV, whereas LDA+DMFT calculations find it at about 2.5 eV. This difference corresponds to what has also recently been found within GW+DMFT, which displays a spectral function very similar to SEx+DDMFT. In these calculations, it was revealed that a pronounced peak in inverse photoemission at 2.7 eV, which in the DMFT literature had been interpreted as the upper Hubbard band of t_{2g} character, is in fact dominantly made up from e_g-states. It was speculated there that the only reason why inverse photoemission has not identified the true upper Hubbard band at 2 eV yet, is its close energetic position to a quite broad quasi-particle peak, together with the very limited resolution of inverse photoemission spectroscopy. Here, we confirm this picture within the new SEx+DDMFT scheme. It will be most interesting to probe the unoccupied part of the spectrum within inverse photoemission spectroscopy in order to locate the 2 eV peak consistently found in GW+DMFT and SEx+DDMFT.

The lower panel of Fig. 1 displays the same spectral function, albeit on a larger energy scale. Here, additional features become visible, namely plasmon replicas at 15 eV and, less pronounced, at around 5 eV. These peaks stem from corresponding features in the frequency-dependent effective Hubbard interactions, encoding the presence of collective plasma oscillations [18].

The momentum-resolved spectral function within screened exchange dynamical mean field theory is shown in Fig. 2, along with the LDA band structure and the band structure obtained from the screened exchange Hamiltonian. The central feature is the dispersing quasi-particle band which has undergone a band renormalization of roughly a factor of 2. Indeed, the bottom of the band at the Γ point is found at about -0.5 eV binding energy, in agreement with angle-resolved photoemission data [34]. We determine the quasi-particle weight corresponding to the DMFT self-energy as $Z^{-1} = 1 - \frac{\partial \Sigma_{DMFT}(i\omega)}{\partial i\omega}$ and find a value of 0.5. This reduction of spectral weight goes hand in hand with a transfer to higher energies, and the lower [upper] Hubbard bands are indeed clearly distinguished in particular at those k-points, where the quasi-particle bands are occupied [empty]. As expected from the k-integrated spectra, the upper Hubbard band is located at around 2 eV, whereas the lower one is found between -1 and -2 eV.

Also plotted are the LDA Kohn-Sham band structure, and the eigenvalues of the screened exchange Hamiltonian H_0. Here, interesting effects of the screened exchange are identified. As usual, exchange tends to widen the band [43, 44], however, as recently also found in GW+DMFT spectra, this effect is larger in the unoccu-

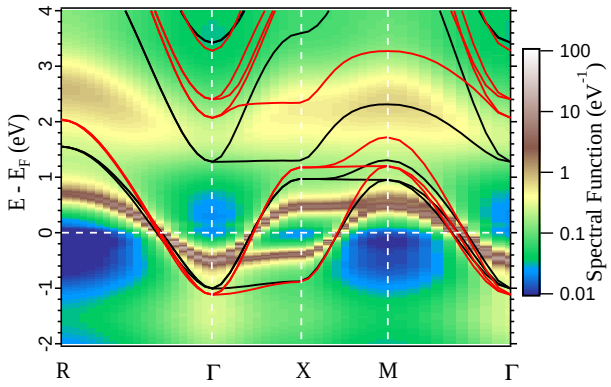

Fig. 2: Spectral function of the t_{2g} states of $SrVO_3$ within screened exchange dynamical mean field theory. Superimposed are the LDA band structure (black lines), and the screened exchange band structure (red lines).

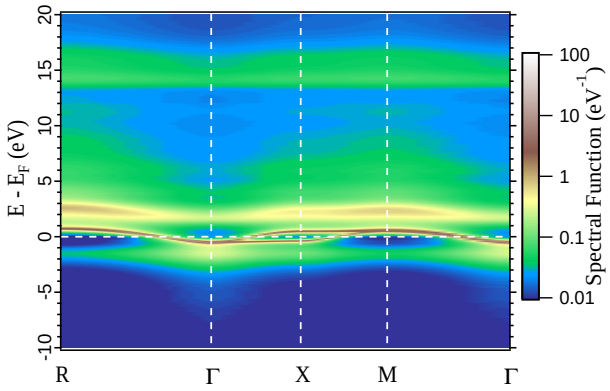

Fig. 3: Spectral function of the t_{2g} states of $SrVO_3$ within screened exchange dynamical mean field theory, as in Fig. 2, but on a larger energy scale.

pied part of the spectrum. For this reason, GW+DMFT and SEx+DDMFT spectra are close to LDA+DMFT ones in their occupied parts, whereas larger corrections are obtained for empty states. In Fig. 3, we plot the momentum-resolved spectral function on a larger energy scale, where also the high-energy plasmon at 15 eV can be clearly distinguished.

Electron-doped SrTiO3 Finally, we discuss a most interesting implication of our theory for weakly correlated materials. Indeed, both screened exchange and the dynamical tail of an otherwise irrelevant Hubbard interaction will still have an effect on the spectral function of a weakly correlated material, the former as a band broadener and the latter as a band narrower, as discussed above. On the example of very lightly electron-doped $SrTiO_3$, we demonstrate that these effects largely cancel and result in a band structure extremely close to the DFT Kohn-Sham one. $SrTiO_3$ is a well-studied band insulator where the only true deficiency of the Kohn-Sham band structure is believed to be the too small band gap opening between oxygen p-states and Ti-3d empty bands. The shape of the latter, however, is largely reproduced even if more advanced theories are applied: the GW approximation offers a band gap correction, without notably modifying the t_{2g} band structure itself [45, 46]. Here, we will be interested neither in the gap nor in the rich physics resulting from electron-lattice coupling in $SrTiO_3$, but rather focus on the band structure of the t_{2g} bands, for which we will show that SEx+DDMFT reproduces to a good approximation the shape and width of the Kohn-Sham bands of DFT. To this effect, we will consider the slightly electron-doped compound, where the t_{2g}-bands are occupied with 0.05 electrons per Ti, and we use the experimental cubic lattice parameter a = 3.905 Å.

In Fig. 4, we compare the LDA band structure for the t_{2g} states to the SEx one and to the band structure for the t_{2g} states resulting from dynamical narrowing effects of the SEx bands. In Ref. [12], it was shown that the effect of the dynamic high-energy tail of the interaction can – in the antiadiabatic limit – be understood in terms of a global band renormalization factor that can directly be calculated from the frequency-dependence of the screened Hubbard interaction: $Z_B = \exp(-\int_0^{+\infty} d\omega \Im U(\omega)/(\pi\omega^2))$. In $SrVO_3$, the value of the bosonic renormalization factor calculated using the interaction from constrained-RPA is $Z_B = 0.7$ [12]. The value we calculate for electron-doped $SrTiO_3$ (with 0.05 electrons) based on the undoped LDA bandstructure on which we apply a chemical potential shift is the same within the numerical precision. While the SEx bandwidth is 1.36 times larger than LDA, after we renormalize the SEx bands by $Z_B = 0.7$ the bandwidth is comparable to LDA. This band structure is in agreement with the experimental inverse photoemission spectrum, which displays a peak around 1.7–2.0 eV [47–50] corresponding to the flat band along the XM direction. The band structure of lightly electron-doped $SrTiO_3$ has also been measured by angle-resolved photoemission in Ref. [51, 52] and the estimates of the effective masses along the ΓX direction – $0.7m_e$-$1.2m_e$ for the light electrons and $7.0m_e$-$20m_e$ for the heavy electrons – are consistent with the LDA band dispersion at the bottom of the bands, further confirming the above picture.

These results indicate that at this very low doping level electron-electron scattering due to the instantaneous part of the Hubbard interaction is negligible, and the width and shape of the band is essentially determined by the counteracting effects of screened exchange and dynamical screening. We now turn to the full SEx+DDMFT calculation for this lightly electron-doped $SrTiO_3$, see colored background of Fig. 4, which indeed confirms this scenario: the maxima of the spectral function correspond to the SEx bands renormalized by Z_B ("SEx+Z_B"). The case of electron-doped $SrTiO_3$ thus strongly suggests that the remarkable performance of LDA in the weakly correlated regime is largely due to to error cancellations between non-

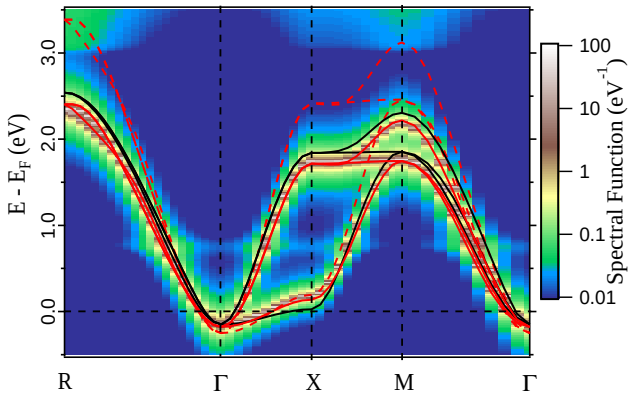

Fig. 4: Band structure of the t_{2g} states of $SrTiO_3$ within LDA (black lines), Screened Exchange (red dashes) and SEx renormalized by a plasmonic factor $Z_B = 0.7$ (red lines) superimposed on the SEx+DDMFT t_{2g} spectral function. The chemical potential corresponds to $n = 0.05$ electron doping per Ti atom, which gives a self-consistent Thomas-Fermi screening wavevector of $k_{TF} = 0.6\ a_0^{-1}$ according to the SEx density of states.

local exchange and dynamical screening effects.

However, while the LDA bandstructure seems to portray relatively well the quasiparticles dispersions, the underlying physics is somewhat simplistic: the reduction of the low-energy spectral weight which necessarily accompanies the band renormalization by Z_B is beyond the LDA, and the description of the high-energy plasmonic excitations – seen for instance in $SrTiO_3$ [47,53] – requires a full SEx+DDMFT calculation.

Conclusion and perspectives. – We have performed combined screened exchange dynamical mean field calculations for the ternary transition metal oxides $SrVO_3$ and electron-doped $SrTiO_3$. The results for $SrVO_3$ are consistent with full GW+DMFT calculations [18]. In particular, we confirm here a pronounced band widening effect on the unoccupied part of the spectrum by the screened exchange part of the Hamiltonian. The final spectral function after the DMFT calculation resembles the one of standard LDA+DMFT calculations in the occupied part of the spectrum, but substantial modifications are obtained in the conduction band. It will be most interesting to probe empty states of $SrVO_3$ – and more generally of correlated materials – within momentum-resolved spectroscopic probes to confirm these findings.

In lightly electron-doped $SrTiO_3$, we have shown how the theory reduces to a band picture given that the dynamical tail can be integrated in the formation of electronic polarons and that the probability of double occupancy at this low filling level is negligible. The antagonistic effects of the non-local screened exchange and of the high-frequency tail of the Hubbard interaction are such that the quasiparticles dispersions are close to the DFT-LDA result. Still, the underlying physics of plasmonic excitations is ignored in LDA, in contrast to our SEx+DDMFT scheme. Our findings shed light on the apparent success not only of combined LDA+DMFT techniques, but also of the Kohn-Sham band structure itself, when used as an approximation to excitation energies for materials with weak electronic Coulomb correlations.

* * *

We acknowledge useful discussions with R. Claessen, I. Mazin, A. Santander, and the authors of Ref. [22] and [18], in particular Thomas Ayral, Michel Ferrero and Olivier Parcollet for support and development of the TRIQS toolkit [24]. This work was supported by IDRIS/GENCI Orsay under project 091393, the National Science Foundation under Grant No. NSF PHY11-25915, and the European Research Council under project 617196.

REFERENCES

[1] Lichtenstein A. I. and Katsnelson M. I., *Phys. Rev. B*, **57** (1998) 6884.
[2] Anisimov V. I., Poteryaev A., Korotin M., Anokhin A. and Kotliar G., *J. Phys. Condens. Matter*, **9** (1997) 7359.
[3] Biermann S., *Electronic structure of transition metal compounds: DFT-DMFT approach* in *Encyclopedia of Materials: Science and Technology*, edited by Buschow K. H. J., Cahn R. W., Flemings M. C., Ilschner B. (print), Kramer E. J., Mahajan S. and Veyssière P. (updates), (Elsevier, Oxford) 2006 pp. 1 – 9.
[4] Biermann S., Dallmeyer A., Carbone C., Eberhardt W., Pampuch C., Rader O., Katsnelson M. I. and Lichtenstein A. I., *JETP Letters*, **80** (2004) 612 condmat0112430.
[5] Lichtenstein A. I., Katsnelson M. I. and Kotliar G., *Phys. Rev. Lett.*, **87** (2001) 067205.
[6] Savrasov S. Y., Kotliar G. and Abrahams E., *Nature*, **410** (2001) 793.
[7] Held K., McMahan A. K. and Scalettar R. T., *Phys. Rev. Lett.*, **87** (2001) 276404.
[8] Amadon B., Lechermann F., Georges A., Jollet F., Wehling T. O. and Lichtenstein A. I., *Phys. Rev. B*, **77** (2008) 205112.
[9] Biermann S., Poteryaev A., Lichtenstein A. I. and Georges A., *Phys. Rev. Lett.*, **94** (2005) 026404.
[10] Martins C., Aichhorn M., Vaugier L. and Biermann S., *Phys. Rev. Lett.*, **107** (2011) 266404.
[11] Casula M., Rubtsov A. and Biermann S., *Phys. Rev. B*, **85** (2012) 035115.
[12] Casula M., Werner P., Vaugier L., Aryasetiawan F., Miyake T., Millis A. J. and Biermann S., *Phys. Rev. Lett.*, **109** (2012) 126408.
[13] Werner P., Casula M., Miyake T., Aryasetiawan F., Millis A. J. and Biermann S., *Nature Physics*, **8** (2012) 331.
[14] Biermann S., Aryasetiawan F. and Georges A., *Phys. Rev. Lett.*, **90** (2003) 086402.
[15] Biermann S., Aryasetiawan F. and Georges A., *arXiv preprint cond-mat/0401653, Proceedings of the*

NATO Advanced Research Workshop on "Physics of Spin in Solids: Materials, Methods, and Applications" in Baku, Azerbaijan, Oct. 2003. NATO Science Series II, Kluwer Academic Publishers B.V., (2004) .

[16] Aryasetiawan F., Biermann S. and Georges A., *arXiv preprint cond-mat/0401626, Proceedings of the conference "Coincidence Studies of Surfaces, Thin Films and Nanostructures", Ringberg castle, Sept. 2003*, (2004) .

[17] Tomczak J. M., Casula M., Miyake T., Aryasetiawan F. and Biermann S., *EPL*, **100** (2012) 67001.

[18] Tomczak J. M., Casula M., Miyake T. and Biermann S., *Phys. Rev. B*, **90** (2014) 165138.

[19] Hansmann P., Ayral T., Vaugier L., Werner P. and Biermann S., *Phys. Rev. Lett.*, **110** (2013) 166401.

[20] Taranto C., Kaltak M., Parragh N., Sangiovanni G., Kresse G., Toschi A. and Held K., *Phys. Rev. B*, **88** (2013) 165119.

[21] Sakuma R., Werner P. and Aryasetiawan F., *Phys. Rev. B*, **88** (2013) 235110.

[22] van Roekeghem A., Ayral T., Tomczak J. M., Casula M., Xu N., Ding H., Ferrero M., Parcollet O., Jiang H. and Biermann S., *Phys. Rev. Lett.*, **113** (2014) 266403.

[23] Hedin L., *J. Phys. Condens. Matter*, **11** (1999) R489.

[24] Ferrero M. and Parcollet O., *TRIQS: A toolbox for research on interacting quantum systems* (2011). `http://ipht.cea.fr/triqs`

[25] Jarrell M. and Gubernatic J., *Phys. Rep.*, **269** (1996) 133.

[26] Onoda M., Ohta H. and Nagasawa H., *Solid State Commun.*, **79** (1991) 281 .

[27] Sekiyama A., Fujiwara H., Imada S., Suga S., Eisaki H., Uchida S. I., Takegahara K., Harima H., Saitoh Y., Nekrasov I. A., Keller G., Kondakov D. E., Kozhevnikov A. V., Pruschke T., Held K., Vollhardt D. and Anisimov V. I., *Phys. Rev. Lett.*, **93** (2004) 156402.

[28] Fujimori A., Hase I., Namatame H., Fujishima Y., Tokura Y., Eisaki H., Uchida S., Takegahara K. and de Groot F. M. F., *Phys. Rev. Lett.*, **69** (1992) 1796.

[29] Inoue I., *Electronic states of correlated transition metal oxides: $Ca_{1-x}Sr_xVO_3$ and Sr_2RuO_4* Ph.D. thesis Tokyo University (1998).

[30] Maiti K., Sarma D. D., Rozenberg M. J., Inoue I. H., Makino H., Goto O., Pedio M. and Cimino R., *EPL*, **55** (2001) 246.

[31] Maiti K., Manju U., Ray S., Mahadevan P., Inoue I. H., Carbone C. and Sarma D. D., *Phys. Rev. B*, **73** (2006) 052508.

[32] Eguchi R., Kiss T., Tsuda S., Shimojima T., Mizokami T., Yokoya T., Chainani A., Shin S., Inoue I. H., Togashi T., Watanabe S., Zhang C. Q., Chen C. T., Arita M., Shimada K., Namatame H. and Taniguchi M., *Phys. Rev. Lett.*, **96** (2006) 076402.

[33] Morikawa K., Mizokawa T., Kobayashi K., Fujimori A., Eisaki H., Uchida S., Iga F. and Nishihara Y., *Phys. Rev. B*, **52** (1995) 13711.

[34] Yoshida T., Tanaka K., Yagi H., Ino A., Eisaki H., Fujimori A. and Shen Z.-X., *Phys. Rev. Lett.*, **95** (2005) 146404.

[35] Takizawa M., Minohara M., Kumigashira H., Toyota D., Oshima M., Wadati H., Yoshida T., Fujimori A., Lippmaa M., Kawasaki M., Koinuma H., Sordi G. and Rozenberg M., *Phys. Rev. B*, **80** (2009) 235104.

[36] Yoshimatsu K., Okabe T., Kumigashira H., Okamoto S., Aizaki S., Fujimori A. and Oshima M., *Phys. Rev. Lett.*, **104** (2010) 147601.

[37] Yoshida T., Hashimoto M., Takizawa T., Fujimori A., Kubota M., Ono K. and Eisaki H., *Phys. Rev. B*, **82** (2010) 085119.

[38] Pavarini E., Yamasaki A., Nuss J. and Andersen O. K., *New Journal Of Physics*, **7** (2005) 188.

[39] Ishida H., Wortmann D. and Liebsch A., *Phys. Rev. B*, **73** (2006) 245421.

[40] Anisimov V. I., Kondakov D. E., Kozhevnikov A. V., Nekrasov I. A., Pchelkina Z. V., Allen J. W., Mo S.-K., Kim H.-D., Metcalf P., Suga S., Sekiyama A., Keller G., Leonov I., Ren X. and Vollhardt D., *Phys. Rev. B*, **71** (2005) 125119.

[41] Lee H., Foyevtsova K., Ferber J., Aichhorn M., Jeschke H. O. and Valentí R., *Phys. Rev. B*, **85** (2012) 165103.

[42] Lechermann F., Georges A., Poteryaev A., Biermann S., Posternak M., Yamasaki A. and Andersen O. K., *Phys. Rev. B*, **74** (2006) 125120.

[43] Ashcroft N. and Mermin N., *Solid State Physics* (Saunders College) 1976.

[44] Miyake T., Martins C., Sakuma R. and Aryasetiawan F., *Phys. Rev. B*, **87** (2013) 115110.

[45] Cappellini G., Bouette-Russo S., Amadon B., Noguera C. and Finocchi F., *J. Phys. Condens. Matter*, **12** (2000) 3671.

[46] Hamann D. R. and Vanderbilt D., *Phys. Rev. B*, **79** (2009) 045109.

[47] Tezuka Y., Shin S., Ishii T., Ejima T., Suzuki S. and Sato S., *J. Phys. Soc. Jpn.*, **63** (1994) 347.

[48] Sarma D. D., Barman S. R., Kajueter H. and Kotliar G., *EPL*, **36** (1996) 307.

[49] Higuchi T., Nozawa S., Tsukamoto T., Ishii H., Eguchi R., Tezuka Y., Yamaguchi S., Kanai K. and Shin S., *Phys. Rev. B*, **66** (2002) 153105.

[50] Baba D., Higuchi T., Kakemoto H., Tokura Y., Shin S. and Tsukamoto T., *Jpn. J. Appl. Phys.*, **42** (2003) L837.

[51] Chang Y. J., Bostwick A., Kim Y. S., Horn K. and Rotenberg E., *Phys. Rev. B*, **81** (2010) 235109.

[52] Santander-Syro A. F., Copie O., Kondo T., Fortuna F., Pailhes S., Weht R., Qiu X. G., Bertran F., Nicolaou A., Taleb-Ibrahimi A., Le Fèvre P., Herranz G., Bibes M., Reyren N., Apertet Y., Lecoeur P., Barthélémy A. and Rozenberg M. J., *Nature*, **469** (2011) 189.

[53] Higuchi T., Tsukamoto T., Watanabe M., Grush M. M., Callcott T. A., Perera R. C., Ederer D. L., Tokura Y., Harada Y., Tezuka Y. and Shin S., *Phys. Rev. B*, **60** (1999) 7711.